Contents

Part I

Q-space imaging studies

Chapter 1

Q-space imaging of the healthy cervical spinal cord (I)

In this chapter we investigate accuracy and sensitivity of spinal cord q-space imaging (QSI) metrics in healthy controls and evaluate its potential for clinical application. As discussed above (see Section **??**), various studies on experimental MRI systems have shown that QSI can provide accurate information about microscopic restriction in excised tissue (Assaf et al., 2000; Bar-Shir et al., 2008; Ong et al., 2008). QSI requires an extensive sampling of different q-values in along a single axis. This restricts the number of diffusion gradient directions that can be sampled when scan time is limited. While in most CNS, e.g. in the brain, high angular resolution of gradient directions is required to capture the variety of different fibre direction, this is less of a problem in spinal cord (SC) due its relatively simple white matter structure. Although the conditions for true QSI, such as the short gradient pulse, are impossible to achieve in clinical systems. Despite all it's difficulties, previous proof-of-concept studies have shown the great potential in the assessment of SC white matter and white pathologies in the human brain (Assaf et al., 2002; **?**) and in the spinal cord Farrell et al. (2008).

Following up on the encouraging results of these previous studies, we aim here to study the reproducibility of QSI metrics in the cervical SC on a standard 3T clinical MRI scanner. We also assess QSI measures both in-plane (XY) and parallel to the main SC axis (Z), not presented before. Previous work in in-vitro rat spinal cord by (Ong et al., 2008; Ong & Wehrli, 2010) suggest that QSI parameters correlate with the axon diameter in different white matter regions. Our particular interest here is to explore whether clinical hardware constraints allow to detect the structural differences between gray matter and different ascending and descending white matter tracts of the cervical SC with QSI. We test whether QSI can discriminate between white matter (WM) in the cervical in healthy subjects and compare conventional apparent diffusion coefficient (ADC) measures, both in plane and along the cord. Furthermore we also test whether any combination of QSI derived FWHM and P0 metrics can better distinguish between WM region of interests (ROIs) than the individual metrics alone.

The remainder of this chapter will present data from the following two experiments. This experiment investigated 9 healthy controls that were scanned at the Wellcome Trust Centre for Neuroimaging as part of a pilot study to study the effect of brachial plexus avulsion (and was also used to study neuromyelitis optica (NMO)). Our preliminary findings in healthy controls were submitted for presentation at the Annual Meeting of the International Society of Magnetic Resonance in Medicine and were accepted for oral presentation (Schneider et al., 2011). Following the encouraging results in this first experiment, we reimplemented an improved protocol on the Philips 3T MRI scanner, that was newly installed in in our lab in 2010. The results of a second QSI pilot study using the new protocols comprise the next chapter (Chapter 2).

1.1 Methods

Study design

Twenty right-handed male healthy subjects were recruited (mean age 35±11yrs) to be scanned on a 3T Tim Trio (Siemens Healthcare, Erlangen). Six subjects were recalled for a second scan on a different day to assess intra-subject reproducibility of QSI derived parameters.

Data acquisition

In each subject we perform cardiac-gated high b-value axialDiffusion Weighted Imaging (DWI)(matrix=96x96, b-spline interpolated to 192x192 in image space, FOV=144x144mm^2, slice thickness=5mm, 20 slices, TE=110ms, TR≈4000ms). The QSI set-up is based on parameters found in the most recent clinical QSI study (Farrell et al., 2008). However, our gradient system only allowed maximum diffusion gradient strength ($|G|$) of 23mT/m (Farrell et al. (2008): 60mT/m). To achieve similar q-values is was necessary increase the gradient duration diffusion gradient pulse duration (δ) to 51ms. Reproduction of the protocol was further complicated by a limitation in the scanner software, which only permits b-value to be specified in multiples of 50 m/s^2 and means that q-values can not be exactly linearly spaced. We acquire a total of 32 b-values between 0-3000s/mm2 in three differentDWIdirections: two directions perpendicular (XY) and one parallel (Z) to the main SC axis. The full protocol is given in Table 1.1.

After an initial quality check, we found that the prescription of the axial DWI slices varying largely between different subjects. Figure 1.1 shows two representive cases for correct and incorrect positioning observed in the dataset. QSI is very sensitive to its alignment to the fibre direction as shown e.g. in (Avram et al., 2004) and the variation in slice positioning might overshadow the subtle differences between WM we are interested in. We therefore measure the angulation between imaging plane and SC longitudinal axis as seen on a T2w sagittal scan at C2/C3. We excluded 11 subjects and their subsequent data with where the angle was less than 80° (ideally we assume the axial imagies perfectly perpendicular, i.e 90°)

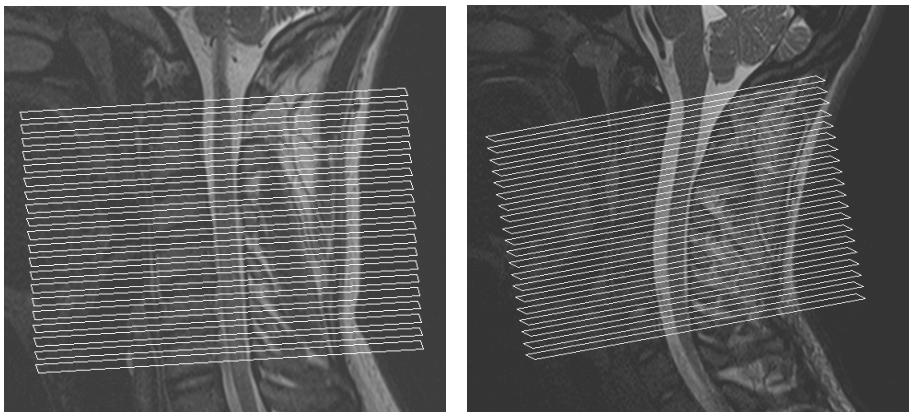

(a) Correct (b) Incorrect

Figure 1.1: Examples of correct and incorrect positioning of QSI scans on sagittal anatomical scans.

Data processing

Similar to Farrell et al. (2008) the two perpendicular diffusion directions were averaged to increase the signal-to-noise ratio. The measurements are linearly regridded to be equidistant in q-space and the displacement probability density function (DPDF) is computed using inverse Fast Fourier Transformation. To increase the resolution of the DPDF, the signal was extrapolated in q-space to a maximum q=166mm^{-1} by fitting a bi-exponential decay curve to theDWIdata as suggested in Cohen & Assaf (2002); Farrell et al. (2008). Figure 1.2 illustrates the processing pipeline. Maps of the full width at half maximum and zero displacement probability were derived for XY and Z as described in Section **??**. For comparison we also computed the apparent diffusion coefficient (see section **??**) from the monoexponential part of the decay curve (b < 1100s/mm2) as in Farrell et al. (2008) for both XY and Z directions using a constrained non-linear least squared fitting algorithm. Figure 1.3 shows both ADC maps and the four QSI parameter maps in one randomly chosen subject.

ROI analysis

We semi-automatically delineate the whole cervical SC area (SCA) between levels C1 and C3 on the b=0 images using the active surface segmentation by Horsfield et al. (2010) available in Jim6. We perform a morphological erosion (2 iterations) of the obtained segmentation mask to exclude voxels with potential partial-volume average effect from surrounding cerebro-spinal fluid (CSF). In addition, four regions of interest were manually placed in specific white matter tracts and one ROI was positioned in the gray matter on all slices between level C1 and C3. The four white matter regions comprised the left and right tracts (l&r-LT) running in the lateral columns and the anterior (AT) and posterior tracts (PT) similar to Hesseltine et al. (2006); Freund et al. (2010) (see Figure 1.4).

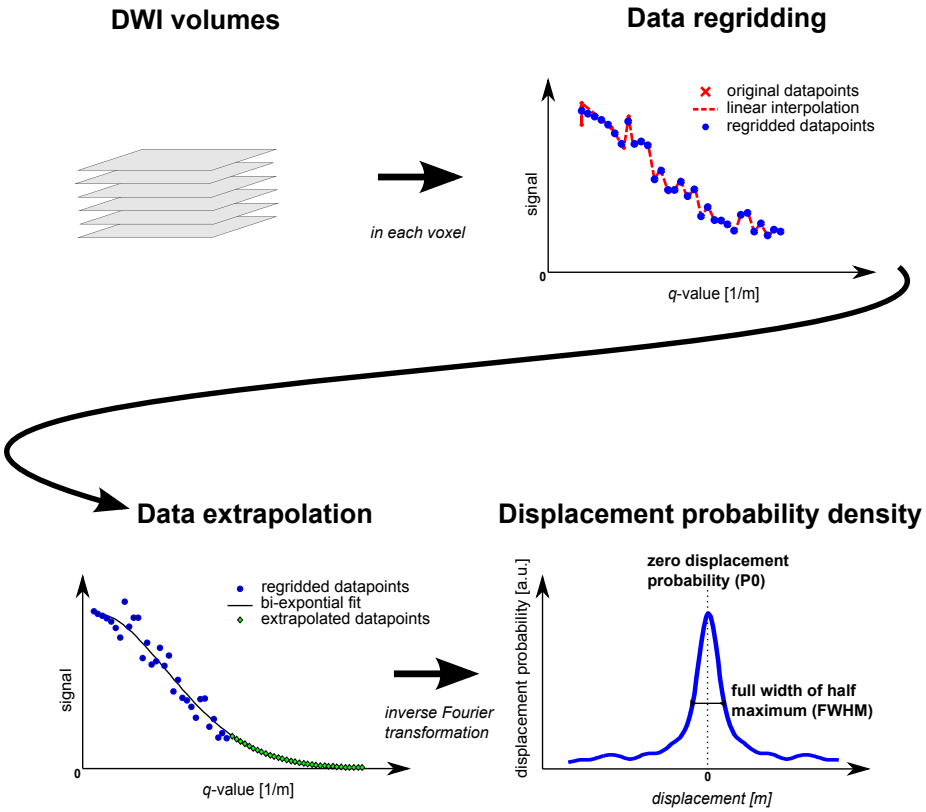

Figure 1.2: Cartoon of the individual steps in our QSI processing pipeline.

Statistical processing

We compare scan/re-scan reproducibility by computing the absolute difference and relative difference in ADC and QSI parameters over the defined ROIs. Further, we investigate the correlation between individual ADC and QSI measurements in XY and Z directions. We pool all voxel-wise measurements over the segmented SC area and compute Pearson's correlation coefficient over all voxels. We test for statistical significant of the correlations with a confidence interval of 95%.

We then compare significant differences in individual metrics using a paired two-tailed t-test and further investigate statisitical significance in the group mean values of the ADC parameters and QSI metrics between tracts by performing the Hotellings-T^2 test (confidence interval=95%). To investigate the relevance of measurements in the different DWI directions, we compute the same significance test of XY-only QSI parameters ($P0_{xy}$, $FWHM_{xy}$) and compare with Z-only ($P0_z$, $FWHM_z$) and the combination of both ($P0_{xy}$, $FWHM_{xy}$, $P0_z$, $FWHM_z$).

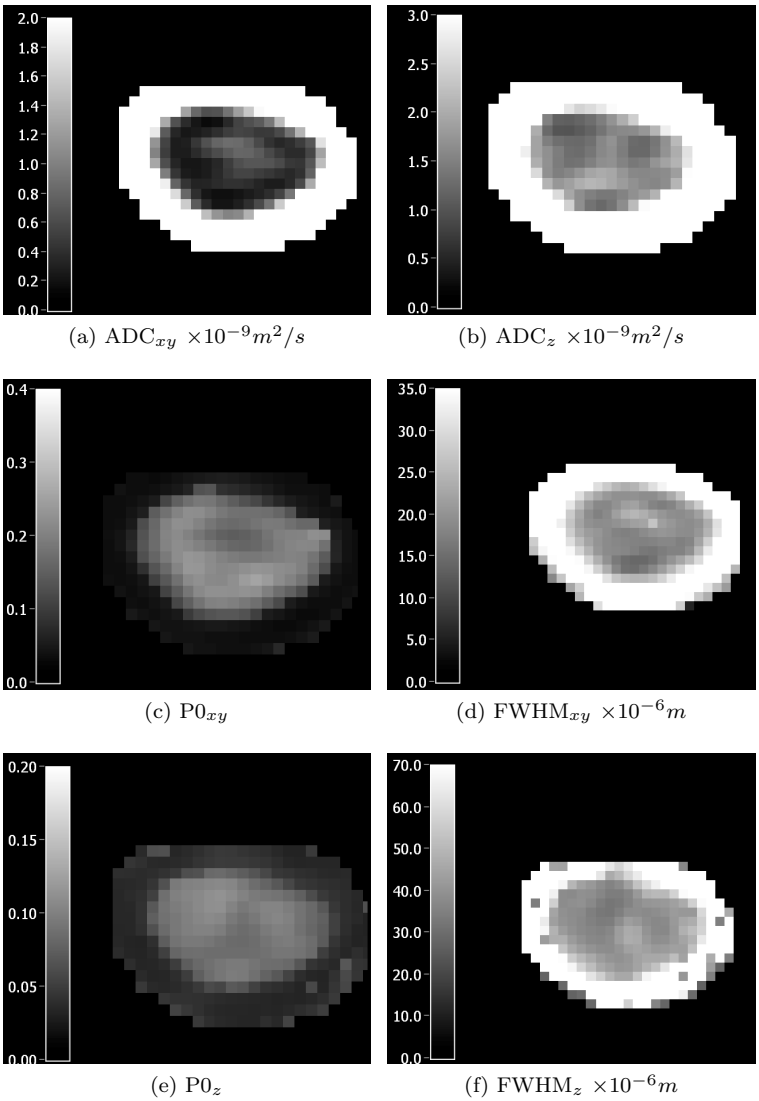

(a) ADC_{xy} $\times 10^{-9} m^2/s$ (b) ADC_z $\times 10^{-9} m^2/s$

(c) $\mathrm{P0}_{xy}$ (d) FWHM_{xy} $\times 10^{-6} m$

(e) $\mathrm{P0}_z$ (f) FWHM_z $\times 10^{-6} m$

Figure 1.3: ADC maps and QSI parameter maps in one exemplary subject at the level of the C2–C3 disc.

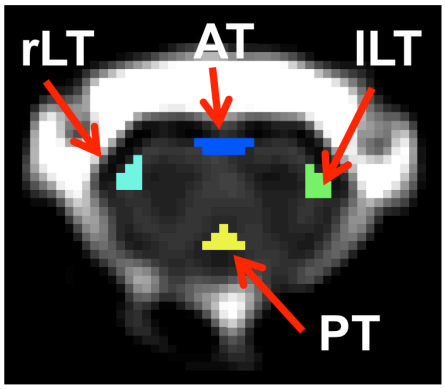

Figure 1.4: Illustration of WM ROIs drawn on b0 image of the cord.

Table 1.1: QSI protocol displaying: Gradient strength (G), q-value (q) and b-value (b) for each of the 32 DWI volumes.

G $[mT/m]$	q $[cm^{-1}]$	b $[s/mm^2]$	G $[mT/m]$	q $[cm^{-1}]$	b $[s/mm^2]$
			... continued		
0.0	0.0	0	0.0	0.0	0
3.0	56.2	50	3.0	56.2	50
4.2	79.4	100	4.2	79.4	100
5.1	97.3	150	5.1	97.3	150
5.9	112.3	200	5.9	112.3	200
6.6	125.6	250	7.8	148.6	350
8.4	158.9	400	9.4	177.6	500
9.8	186.3	550	10.7	202.5	650
11.5	217.5	750	12.2	231.6	850
12.9	244.8	950	13.9	263.4	1100
14.5	275.2	1200	15.4	291.9	1350
15.9	302.5	1450	16.7	317.7	1600
17.5	332.3	1750	18.2	346.2	1900
19.2	364.0	2100	19.9	376.8	2250
20.7	393.2	2450	21.3	405.0	2600
22.2	420.3	2800	22.9	435.1	3000

1.2 Results

Reproducibility

Tables **??** shows absolute and relative differences between scan and rescan of three healthy subjects in ADC_{xy} and ADC_z (1.3a) and QSI metrics in XY and Z direction (1.3b). We observe a general trend of measurements perpendicular to the long SC fibres presenting higher variation between scan and rescan than parallel measurements in ADC and both QSI metrics in all subjects. In particular ADC_{xy} shows very high intra-subject variation between 20–40% on average in all white matter ROIs, while only GM values show good reproducibility value of less than 11% variation. In particular ADC_z appears more reproducible in all three subjects with average relative variation between 5–16%.

The perpendicular QSI metrics $P0_{xy}$ and $FWHM_{xy}$ present good reproducibility values of 6–12% and are up to 4 times lower than ADC_{xy} measurements in corresponding ROIs. In both $P0_z$ and $FWHM_z$ we observe relative change between 4–13% similar to values in ADC_z.

Differences between tract-specific ROI measurements

We compare the average values and standard devation over all 9 subjects between tract-specific ROIs for ADC values in Figure 1.5a and QSI metrics in Figure 1.5. As a general trend, we observe higher inter-subject variation in XY measurements compared to Z measurements among all 9 subjects which is in line with our results of intra-subject variation shown above.

Table 1.3 present p-values for pairwise differences between different tract-ROIs for ADC and QSI metrics. The most noteable differences are found between the GM ROI and the white matter regions in ADC_{xy} and both $P0_{xy}$/$FWHM_{xy}$ with high statistical significance ($p < 0.01$ between WM tracts GM for all QSI_{xy} metrics), while ADC_z and QSI_z metrics are less different between GM ROI and WM ROIs. In fact, significant differences are only found between rLT and GM in ADC_z. The QSI_z metrics only show significant differences between GM and rRT in $P0_z$ (p=0.01) and between GM and AT and PT ($FWHM_z$).

Between WM ROIs only the left LT but not the right LT is significantly different from both AT and PT in ADC_{xy} perpendicular to long white matter fibres. Parallel to the long SC axis we only find ADC_z in the right LT significantly lower from AT and PT. Left and right LT show significant differences in both ADC_{xy} and ADC_z while we find no difference between AT or PT. In QSI metrics we find the same tracts as with ADC to be significantly different in XY and Z direction. However, p-values are increased in QSI compared to corresponding ADC, but remain below $p < 0.05$.

Multi-variate differences between tract-specific ROI measurements

The single parameter comparisions above indicate that both ADC and QSI metrics can discriminate some WM tracts, but offer complementary information in perpendicular and parallel measurements. The multivariate Hotelling's-T^2 allows us to test whether a combination of XY and Z metrics is better suited to

Table 1.2: Absolute and relative change (in percent) between scan and rescan of diffusivities and QSI parameters in 3 healthy volunteers

ADC_{xy} $\times 10^{-9} m^2/s$

subject	rLT	lLT	AT	PT	GM
1	0.10 (30.4%)	0.00 (4.7%)	0.07 (27.6%)	0.06 (24.1%)	0.09 (12.0%)
2	0.06 (16.9%)	0.06 (34.4%)	0.12 (44.6%)	0.03 (11.0%)	0.05 (12.0%)
3	0.09 (25.5%)	0.12 (51.9%)	0.24 (57.2%)	0.20 (82.5%)	0.04 (8.6%)
mean	0.08 (24.3%)	0.06 (30.4%)	0.14 (43.1%)	0.10 (39.2%)	0.06 (10.9%)

ADC_z $\times 10^{-9} m^2/s$

subject	rLT	lLT	AT	PT	GM
1	0.04 (3.3%)	0.07 (4.7%)	0.18 (12.2%)	0.03 (2.1%)	0.03 (2.4%)
2	0.13 (9.0%)	0.17 (9.8%)	0.40 (23.2%)	0.03 (1.6%)	0.30 (16.9%)
3	0.16 (12.5%)	0.10 (6.2%)	0.21 (12.9%)	0.16 (10.2%)	0.28 (16.6%)
mean	0.11 (8.3%)	0.12 (6.9%)	0.26 (16.1%)	0.07 (4.7%)	0.20 (12.0%)

(a) Perpendicular (ADC_{xy}) and parallel diffusivity (ADC_z)

$P0_{xy}$

subject	rLT	lLT	AT	PT	GM
1	0.01 (3.1%)	0.02 (6.8%)	0.01 (3.4%)	0.00 (1.7%)	0.00 (1.9%)
2	0.00 (0.4%)	0.00 (0.3%)	0.01 (4.3%)	0.01 (3.3%)	0.00 (2.3%)
3	0.01 (6.1%)	0.06 (28.2%)	0.04 (19.9%)	0.06 (26.7%)	0.03 (14.8%)
mean	0.01 (3.2%)	0.03 (11.8%)	0.02 (9.2%)	0.02 (10.6%)	0.01 (6.3%)

$FWHM_{xy}$

subject	rLT	lLT	AT	PT	GM
1	0.52 (2.5%)	0.67 (4.8%)	0.67 (3.5%)	0.29 (1.5%)	0.62 (2.4%)
2	0.03 (0.1%)	0.29 (1.6%)	0.76 (4.1%)	0.36 (1.9%)	0.32 (1.5%)
3	1.10 (5.2%)	5.69 (29.6%)	4.72 (20.6%)	5.10 (27.5%)	3.29 (15.5%)
mean	0.55 (2.6%)	2.22 (12.0%)	2.05 (9.4%)	1.92 (10.3%)	1.41 (6.5%)

$P0_z$

subject	rLT	lLT	AT	PT	GM
1	0.00 (4.5%)	0.00 (0.6%)	0.01 (6.9%)	0.00 (2.5%)	0.01 (5.6%)
2	0.01 (9.2%)	0.01 (11.4%)	0.01 (11.0%)	0.00 (3.4%)	0.01 (10.6%)
3	0.01 (6.0%)	0.00 (0.1%)	0.00 (1.2%)	0.01 (7.8%)	0.01 (14.9%)
mean	0.01 (6.6%)	0.00 (4.1%)	0.01 (6.3%)	0.00 (4.6%)	0.01 (10.4%)

$FWHM_z$

subject	rLT	lLT	AT	PT	GM
1	1.42 (3.9%)	1.67 (3.9%)	4.20 (10.4%)	1.07 (2.7%)	3.86 (10.7%)
2	5.72 (15.4%)	9.04 (22.2%)	4.69 (11.6%)	4.47 (10.9%)	4.76 (12.5%)
3	1.08 (3.0%)	0.13 (0.3%)	1.66 (4.1%)	4.89 (12.4%)	6.17 (16.1%)
mean	2.74 (7.4%)	3.61 (8.8%)	3.52 (8.7%)	3.48 (8.6%)	4.93 (13.1%)

(b) Perpendicular and parallel QSI parameters

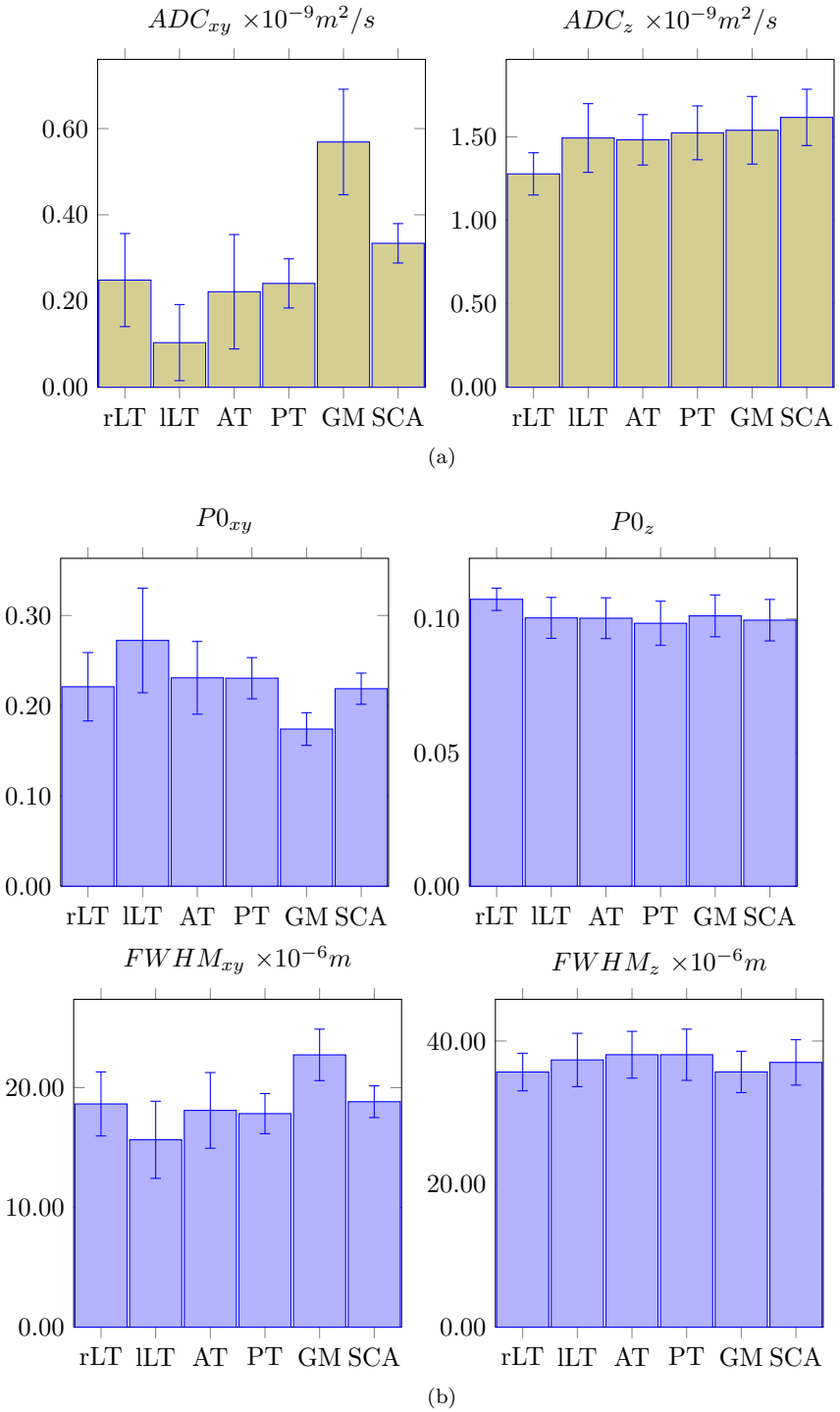

Figure 1.5: Mean and standard deviation of perpendicular and parallel ADC and QSI metrics for all ROIs over all 9 volunteers.

Table 1.3: Significance of pair-wise differences between SC tracts in diffusivities and QSI parameters (confidence interval: 95%). Statistically significant differences are marked as follows: **bold** if $p < 0.05$, ***bold-italic*** if $p < 0.01$.

$\mathbf{ADC}_{xy} \times 10^{-9} m^2/s$	lLT	AT	PT	GM
rLT	**0.01**	0.60	0.84	***<0.01***
lLT		***<0.01***	***<0.01***	***<0.01***
AT			0.56	***<0.01***
PT				***<0.01***

$\mathbf{ADC}_{z} \times 10^{-9} m^2/s$	lLT	AT	PT	GM
rLT	**0.01**	***<0.01***	***<0.01***	***<0.01***
lLT		0.85	***<0.01***	0.57
AT			0.44	0.30
PT				0.74

(a)

$\mathbf{P0}_{xy}$	lLT	AT	PT	GM
rLT	**0.04**	0.27	0.48	***<0.01***
lLT		**0.05**	0.48	***<0.01***
AT			0.97	***<0.01***
PT				***<0.01***

$\mathbf{P0}_{z}$	lLT	AT	PT	GM
rLT	**0.01**	***<0.01***	***<0.01***	**0.01**
lLT		0.94	***<0.01***	0.77
AT			0.40	0.69
PT				0.16

$\mathbf{FWHM}_{xy}$	lLT	AT	PT	GM
rLT	**0.04**	0.56	0.37	***<0.01***
lLT		**0.02**	0.37	***<0.01***
AT			0.72	**0.01**
PT				***<0.01***

$\mathbf{FWHM}_{z}$	lLT	AT	PT	GM
rLT	0.21	**0.02**	**0.03**	0.99
lLT		0.20	**0.03**	0.13
AT			1.00	**0.01**
PT				**0.01**

(b)

characterize and discriminate WM measures in different ROIs. In the following, we present results for the following combinations of parameters:

- Both diffusivity parameters ADC_{xy} and ADC_{z} (Table 1.5a)
- Perpendicular only QSI metrics $\mathrm{P0}_{xy}$ and FWHM_{xy} (Table 1.5a)
- Parallel only QSI metrics $\mathrm{P0}_{z}$ and FWHM_{z} (Table 1.5c)
- Perpendicular and parallel QSI metrics $\mathrm{P0}_{xy}$, FWHM_{xy}, $\mathrm{P0}_{z}$ and FWHM_{z} (Table 1.5d)

Similar to the single t-test results shown above, GM and WM ROIs can clearly be distinguished using either of the combinations of ADC and QSI parameters. However, GM/WM differences are more pronounced in XY than in Z direction. The combined ADC metrics show significant differences between the both lateral tracts and also l/r LT and the posterior WM ROI. AT is only significantly different from the right but not the left LT.

For combination of QSI parameters in Z only as well as the combination of both XY and Z, the only two emerging differences are found between lLT/rLT and rLT/PT, both with $p < 0.05$.

Table 1.4: Hotelling's-T^2 significance of pair-wise tract-specific differences for ADC and QSI parameters. (**bold** marks $p < 0.05$, ***bold-italic*** marks $p < 0.01$).

	lLT	AT	PT	GM
rLT	***<0.01***	**0.02**	**0.01**	***<0.01***
lLT		0.10	**0.01**	***<0.01***
AT			0.85	***<0.01***
PT				***<0.01***

(a) Combined ADC_{xy},ADC_z

	lLT	AT	PT	GM
rLT	0.13	0.79	0.71	**0.01**
lLT		0.26	0.12	***<0.01***
AT			0.76	**0.02**
PT				***<0.01***

(b) Combined perpendicular QSI parameters ($P0_{xy}$,$FWHM_{xy}$)

	lLT	AT	PT	GM
rLT	**0.03**	0.08	**0.02**	**0.02**
lLT		0.60	0.86	0.18
AT			0.49	**0.01**
PT				***<0.01***

(c) Combined parallel QSI parameters ($P0_z$,$FWHM_z$)

	lLT	AT	PT	GM
rLT	**0.04**	0.25	**0.01**	***<0.01***
lLT		0.62	0.50	***<0.01***
AT			0.75	***<0.01***
PT				***<0.01***

(d) Combined perpendicular and parallel QSI parameters ($P0_{xy}$,$FWHM_{xy}$,$P0_z$,$FWHM_z$)

Voxel-wise correlation of ADC and QSI metrics

Table 1.5 shows the Pearson correlation coefficient r and statistical significance of the correlation between ADC and QSI parameters over all SC voxels in all subjects. We observe significant correlations between ADC_{xy} and ADC_z. Further we find significant correlations between and QSI parameters both within and across XY and Z direction. Interestingly, we find both $FWHM_{xy}$ and $P0_z$ are correlated with each other and also with both ADC parameters, while the other two QSI parameters $P0_{xy}$ and $FWHM_z$ did neither correlate with each other nor any other metrics.

1.3 Discussion

QSI metrics obtained without sequence development, using standardDWIprotocol available on a 3T clinical scanner, show a good reproducibility that is superior to simple ADC analysis. We observe tract-specific correlations between ADC and QSI parameters between several WM tracts. However some of the associations in QSI metrics are weaker in XY compared to Z, particularly between lateral and posterior tracts. Together with the findings of weak of correlation between QSI and ADC metrics in both XY and Z, our results suggest that the Z direction provides additional information to perpendicular measurements. Our results also suggest that on a clinical scanner QSI might not be able to reliably distinguish between individual WM tracts.

The results of this experiment need to be interpreted with caution due to the limitations in hardware and software in the experimental setup. In particular the low gradient strength used in this study might conceal differences between tracts. Simulations by Lätt et al. (2007) show that insufficient gradient strength

Table 1.5: Pearson-correlation coefficient and significance between all ADC and QSI metrics. The p-values < 0.01 are marked bold-italic.

		ADC_{xy}	ADC_z	$P0_{xy}$	$FWHM_{xy}$	$P0_z$	$FWHM_z$
ADC_{xy}	r		0.58	0.00	-0.74	0.20	0.01
	p		***<0.01***	0.91	***<0.01***	***<0.01***	0.56
ADC_z	r	0.58		0.00	-0.29	0.71	0.00
	p	***<0.01***		0.87	***<0.01***	***<0.01***	0.82
$P0_{xy}$	r	0.00	0.00		0.00	0.00	0.00
	p & 0.91	0.87		0.82	0.99	1.00	
$FWHM_{xy}$	r	-0.74	-0.29	0.00		-0.18	-0.01
	p	***<0.01***	***<0.01***	0.82		***<0.01***	0.70
$P0_z$	r	0.20	0.71	0.00	-0.18		0.01
	p	***<0.01***	***<0.01***	0.99	***<0.01***		0.52
$FWHM_z$	r	0.01	0.00	0.00	-0.01	0.01	
	p	0.56	0.82	1.00	0.70	0.52	

might lead to overestimation of compartment size and suggest that gradients of at least 60 mT/m are required to be sensitive to the typical size of axons found in human WM. Beside the hardware limitations of the scanner, there are also several issues in the design of this study including:

1. the high number of subjects that had to be excluded due to misalignment of the axial images
2. the linear regridding that made necessary because of scanner software limitation
3. the relative high in-plane resolution of the acquired images

To overcome these flaws in the study design, the data had to undergo a rather extensive pre-processing pipeline, which might weaken the confidence in our results. The installation of a new 3T scanner in our lab offered us the possibility to repeat this experiment with improved hardware and software capabilities. The results are described in the following chapter.

Chapter 2

Q-space imaging of the healthy cervical spinal cord (II)

The aim of this study is to repeat the experiment in Chapter 1 and improve on the several confounding factors in we identified the previous chapter. We carefully optimise the acquisition to achieve an increase in spatial resolution and signal-to-noise ratio of the axial DWI measurements, and higher diffusion gradient strength as well as linear spacing of q-values.

2.1 Methods

Study design

We recruit 10 healthy volunteers (4 male/6 female) to be scanned on a 3T Philips Achieva 3TX (Philips Healthcare, Eindhoven). Four subjects are rescanned at a different time to assess intra-subject reproducibility of the derived parameters.

Data acquisition

To ensure consistent positioning of the DWI columes among all scans, we acquire a structural scan of the whole cervical cord using a sagittal T2 weighted turbo-spin-echo sequence (voxel size=1x1x3 mm^3, FOV=256x247mm^2, TR=4000ms, TE=63ms, 2 averages). We then position the DWI images based on the structural scan so that the centre of the acquisitions volume is aligned with the C2/C3 disc and the acquisition plane is parallel to the cord at this level.

We use a cardiac gated DWI acquisition with the following imaging parameters: voxel size=1x1x5 mm^3, FOV=64x64mm^2, TR=9RR, TE=129ms). To avoid aliasing artifacts from surrounding tissue we use a ZOOM sequence with outer-volume suppression as described in (Wilm et al., 2007). We acquire 32 DWI equally spaced q-values in two directions perpendicular (XY) and in one parallel (Z) direction with respect to the main SC axis. To achieve the maximum possible gradient strength on our scanner we exploit the combination of parallel

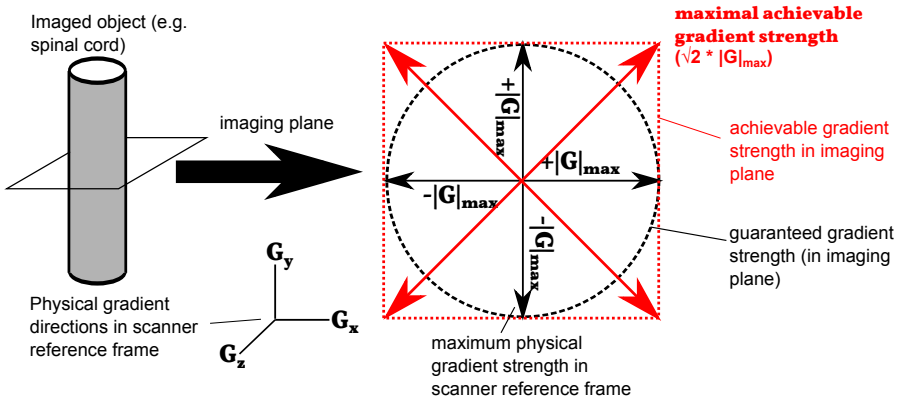

Figure 2.1: Cartoon of our implemented gradient strength modification method.

gradient amplifiers in our scanner, which each can generate a maximum $|G|$ of 62mT/m in the along the major axes of the scanner bore. Assuming axial symmetry of the axons along the long axis of the spinal cord, we modify the scanner software to drive multiple gradient amplifiers in two orthogonal directions perpendicular to major SC fibre direction (see Figure 2.1 for illustration). This allows us to generate a guaranteed maximum $|G|$ of $\sqrt{2} * 62mT/m = 87mT/m$ in XY direction. In Z direction we use a maximum $|G|$ of 62 mT/m. We use the same q-values in this experiment as described in Farrell et al. (2008). However the increase in $|G|$ allows us to reduce the gradient duration from 50ms to 11.4ms in XY direction (16ms in Z). The full protocol is given in Table 2.1.

Data processing & analysis

We apply the same data processing pipeline as in the previous experiment (see Section 1.1) with the exception of the linear regridding of acquired q-values, which is not necessary in this data set. We segment the whole cervical SC and place ROIs in the lateral columns and the anterior and posterior tracts between level C1/2 and C3 in all subjects (refer to Figure 1.4 for an illustration of the drawn ROIs).

Statistical processing

We derive the same statistics from this dataset as in the previous chapter. We present the absolute difference and relative difference in ADC and QSI parameters over the defined ROIs in the scan/re-scan cases. Further we show results of t-tests between different tracts for individual metrics and the multivariate Hotelling-T^2 test for combination of parameters. We also investigate voxel-wise correlations between the six metrics using Pearson correlation coefficient.

Table 2.1: QSI protocol displaying: Gradient strength (G), q-value (q) and b-value (b) for each of the 32 DWI volumes.

			... continued		
G $[mT/m]$	q $[cm^{-1}]$	b $[s/mm^2]$	G $[mT/m]$	q $[cm^{-1}]$	b $[s/mm^2]$
0.0	0.0	0	0.0	0.0	0
5.8	66.2	22	2.9	33.0	6
11.7	132.8	90	8.7	99.2	50
17.5	198.6	200	14.6	165.7	139
23.3	264.5	355	20.4	231.5	272
29.1	330.3	554	26.2	297.4	449
35.0	397.3	802	32.1	364.3	674
40.8	463.1	1089	37.9	430.2	940
46.6	528.9	1421	43.7	496.0	1250
52.5	595.9	1803	49.5	561.8	1603
58.3	661.7	2224	55.4	628.8	2008
64.1	727.5	2688	61.2	694.6	2451
69.9	793.4	3197	67	760.5	2937
75.8	860.3	3759	72.9	827.4	3477
81.6	926.2	4357	78.7	893.2	4053
87.4	992.0	4998	84.5	959.1	4672

(a) Protocol for X and Y direction

			... continued		
G $[mT/m]$	q $[cm^{-1}]$	b $[s/mm^2]$	G $[mT/m]$	q $[cm^{-1}]$	b $[s/mm^2]$
0.0	0.0	0	0.0	0.0	0
4.1	46.9	11	2.1	23.4	3
8.3	94.2	45	6.2	70.4	25
12.4	140.9	101	10.4	117.5	70
16.5	187.6	179	14.5	164.2	137
20.6	234.2	279	18.6	210.9	226
24.8	281.7	403	22.8	258.4	339
28.9	328.4	548	26.9	305.1	473
33.0	375.1	715	31.0	351.8	629
37.2	422.6	907	35.1	398.5	806
41.3	469.3	1119	39.3	446.0	1010
45.5	516.0	1352	43.4	492.6	1233
49.6	562.7	1608	47.5	539.3	1477
53.8	610.2	1891	51.7	586.8	1749
57.9	656.9	2191	55.8	633.5	2038
62.0	703.5	2514	59.9	680.2	2350

(b) Protocol for Z direction

2.2 Results

Scan/Rescan reproducibility

Table 2.2 shows the intra-subject variability for ADC and QSI metrics in all five subjects. In both ADC and QSI and all ROIs, the observed COV values are lower in Z compared to the XY direction. We also observe that QSI metrics are generally more reproducible than ADC values. The small relative change between scan/rescan values for QSI metrics suggest very good reproducibility in both XY (less than 10%) and Z (less than 5%), while the intra-subject variation of ADC values is considerably higher with 26% in XY and 7% in Z. All investigated ROIs show similar scan/rescan reproducibility over all the studied ADC and QSI parameters.

Differences between tract-specific ROI measurements

Comparing XY and Z parameters Figure 2.2 shows mean and standard deviation of both ADC and QSI values over all 10 healthy subjects in each ROI. In all ROIs, ADC_{xy} values are significantly lower than ADC_z. Similarly, in XY we also observe small FWHM and larger P0 compared to Z parameters. Both ADC and QSI findings support our assumption of restricted diffusion predominantly in XY direction.

Difference between WM and GM Table 2.3 presents the results of pairwise t-tests between all GM and WM ROIs, testing for for statistically significant differences in individual ADC and QSI metrics. The most significant differences are found between both the lateral tracts and GM region, as well as the posterior tract and GM. In both ADC and QSI, the XY measurements distinguish WM and GM regions better than the Z parameters. All the XY parameters, i.e. ADC_{xy}, $P0_{xy}$ and $FWHM_{xy}$, show similar p-values in detecting the differences between GM and the WM regions. In contrast, neither of the parameters is able to discriminate AT from GM.

Differences between WM regions No statistical difference is observed between left and right LT in neither ADC or QSI values. However, we detect differences between the PT and both LTs with ADC and QSI ($p<0.05$). The $P-values$ between PT and LTs are consistently smaller in $P0_{xy}$ and $FWHM_{xy}$ compared to ADC_{xy}. None of these tracts show significant differences in any of the XY metrics. AT appears different from all the other WM regions with most ADC/QSI parameters in XY and Z.

Multi-variate differences between tract-specific ROI measurements Table 2.4 shows the results of the multivariate test for statistical differences between ROIs for various combinations of ADC_{xy}, ADC_z, and P0 and FWHM metrics in XY and Z. As expected from single parameter t-test results, either tested combination is sensitive to differences between WM (except AT) and GM. However, including any of the QSI_z parameters noticably reduced the significance of the found differences.

Table 2.2: Absolute and relative change (in percent) between scan and rescan of ADC and QSI in 4 healthy volunteers

ADC_{xy} $\times 10^{-9} m^2/s$

subject	rLT	lLT	AT	PT	GM
1	0.02 (7.6%)	0.04 (11.5%)	0.01 (1.9%)	0.03 (9.5%)	0.01 (1.0%)
2	0.03 (10.1%)	0.10 (34.9%)	0.07 (15.0%)	0.21 (47.3%)	0.01 (3.0%)
3	0.02 (6.5%)	0.09 (24.4%)	0.09 (18.6%)	0.13 (37.5%)	0.08 (14.8%)
4	0.11 (29.8%)	0.06 (16.4%)	0.17 (32.1%)	0.03 (10.4%)	0.03 (5.3%)
mean	0.05 (13.5%)	0.07 (21.8%)	0.08 (16.9%)	0.10 (26.2%)	0.03 (6.0%)

ADC_z $\times 10^{-9} m^2/s$

subject	rLT	lLT	AT	PT	GM
1	0.22 (10.9%)	0.07 (3.4%)	0.23 (12.3%)	0.24 (11.9%)	0.31 (19.9%)
2	0.33 (17.4%)	0.12 (5.9%)	0.23 (14.0%)	0.32 (14.3%)	0.34 (17.6%)
3	0.18 (9.3%)	0.01 (0.4%)	0.05 (2.6%)	0.03 (1.3%)	0.04 (2.1%)
4	0.19 (9.5%)	0.05 (2.7%)	0.01 (0.6%)	0.12 (5.6%)	0.13 (7.4%)
mean	0.23 (11.8%)	0.06 (3.1%)	0.13 (7.4%)	0.18 (8.3%)	0.21 (11.8%)

(a)

$P0_{xy}$

subject	rLT	lLT	AT	PT	GM
1	0.00 (0.0%)	0.04 (18.4%)	0.02 (8.6%)	0.00 (1.8%)	0.00 (2.5%)
2	0.00 (0.0%)	0.03 (11.1%)	0.01 (4.4%)	0.03 (15.8%)	0.01 (3.2%)
3	0.01 (5.7%)	0.00 (0.0%)	0.01 (4.7%)	0.02 (10.6%)	0.02 (10.9%)
4	0.01 (3.8%)	0.01 (3.4%)	0.00 (2.2%)	0.00 (0.0%)	0.01 (4.0%)
mean	0.01 (0.0%)	0.02 (0.0%)	0.01 (0.0%)	0.01 (0.0%)	0.01 (0.0%)

$FWHM_{xy}$

subject	rLT	lLT	AT	PT	GM
1	0.00 (0.0%)	3.00 (14.6%)	1.60 (7.1%)	0.40 (1.9%)	0.70 (2.5%)
2	0.20 (0.9%)	1.90 (9.4%)	1.00 (4.0%)	3.20 (13.6%)	1.00 (4.7%)
3	1.20 (5.9%)	0.30 (1.4%)	0.50 (2.1%)	2.00 (9.3%)	1.90 (7.6%)
4	0.40 (1.8%)	0.10 (0.4%)	0.10 (0.4%)	0.40 (1.8%)	0.80 (3.1%)
mean	0.45 (2.2%)	1.33 (6.5%)	0.80 (3.4%)	1.50 (6.7%)	1.10 (4.5%)

$P0_z$

subject	rLT	lLT	AT	PT	GM
1	0.01 (4.8%)	0.00 (2.9%)	0.01 (4.6%)	0.01 (7.5%)	0.01 (10.1%)
2	0.01 (11.1%)	0.00 (2.0%)	0.01 (7.0%)	0.01 (5.8%)	0.01 (10.9%)
3	0.01 (5.7%)	0.00 (1.2%)	0.00 (1.9%)	0.00 (0.4%)	0.00 (1.0%)
4	0.01 (5.9%)	0.00 (0.0%)	0.00 (0.9%)	0.00 (3.1%)	0.00 (3.6%)
mean	0.01 (6.9%)	0.00 (1.5%)	0.00 (3.6%)	0.00 (4.2%)	0.01 (6.4%)

$FWHM_z$

subject	rLT	lLT	AT	PT	GM
1	1.80 (3.0%)	1.00 (1.6%)	3.00 (5.3%)	5.40 (8.8%)	4.40 (8.4%)
2	6.10 (10.4%)	0.80 (1.3%)	3.50 (6.4%)	4.30 (6.5%)	8.50 (14.1%)
3	4.20 (7.1%)	1.20 (1.8%)	1.60 (2.7%)	0.40 (0.6%)	1.60 (2.6%)
4	3.50 (5.6%)	1.00 (1.7%)	0.50 (0.9%)	0.00 (0.0%)	1.60 (2.8%)
mean	3.90 (6.5%)	1.00 (1.6%)	2.15 (3.8%)	2.53 (4.0%)	4.03 (7.0%)

(b)

Table 2.3: Pair-wise t-test results between SC tracts in ADC and QSI parameters. Statiscally different values are marked **bold** for p<0.05, ***bold-italic*** for p<0.01.

ADC$_{xy}$	lLT	AT	PT	GM
rLT	0.51	***<0.01***	0.53	***<0.01***
lLT		***<0.01***	0.60	***<0.01***
AT			**0.03**	0.73
PT				**0.02**

ADC$_z$	lLT	AT	PT	GM
rLT	0.83	0.06	**0.03**	**0.02**
lLT		**0.01**	0.06	***<0.01***
AT			***<0.01***	0.44
PT				***<0.01***

(a) ADC$_{xy}$& ADC$_z$

P0$_{xy}$	lLT	AT	PT	GM
rLT	0.96	***<0.01***	0.82	***<0.01***
lLT		***<0.01***	0.83	***<0.01***
AT			***<0.01***	0.36
PT				**0.01**

FWHM$_{xy}$	lLT	AT	PT	GM
rLT	0.50	***<0.01***	0.58	***<0.01***
lLT		***<0.01***	0.91	***<0.01***
AT			***<0.01***	0.24
PT				***<0.01***

P0$_z$	lLT	AT	PT	GM
rLT	0.93	0.06	**0.02**	0.05
lLT		***<0.01***	0.05	**0.01**
AT			***<0.01***	0.74
PT				***<0.01***

FWHM$_z$	lLT	AT	PT	GM
rLT	0.46	0.12	***<0.01***	0.19
lLT		**0.01**	**0.03**	**0.04**
AT			***<0.01***	0.85
PT				***<0.01***

(b) QSI$_{xy}$& QSI$_z$ metrics

Between WM regions, the combination of ADC$_{xy}$ and ADC$_z$) good discrimination between the left and right LTs and the PT. In contrast, neither combinations of QSI metrics in XY is significantly different between any pair of WM regions. However, the combined QSI$_z$ metrics (P0$_z$,FWHM$_z$) revealed differences between PT and rLT and PT and AT that are not found in XY. The full combination of both QSI$_{xy}$ and QSI$_z$ revealed the least differences between any tracts.

Correlation between ADC and QSI

Table 2.5 shows the Pearson coefficient and p-value for voxel-wise correlations between the investigated ADC and QSI metrics. We observe a strong correspondence (p<0.01) between ADC measurements and P0 and FWMH QSI metrics in X as well as FWHM in Z. P0$_z$ is the only parameter that does not correlate with any of the other metrics, suggesting additional information that is neither captured in the ADC$_z$ value nor captured with any of the XY measurements.

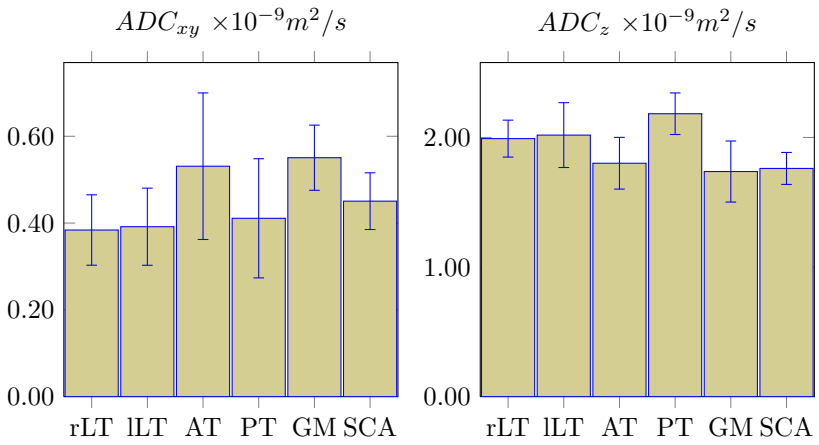

(a) ADC_{xy}& ADC_z

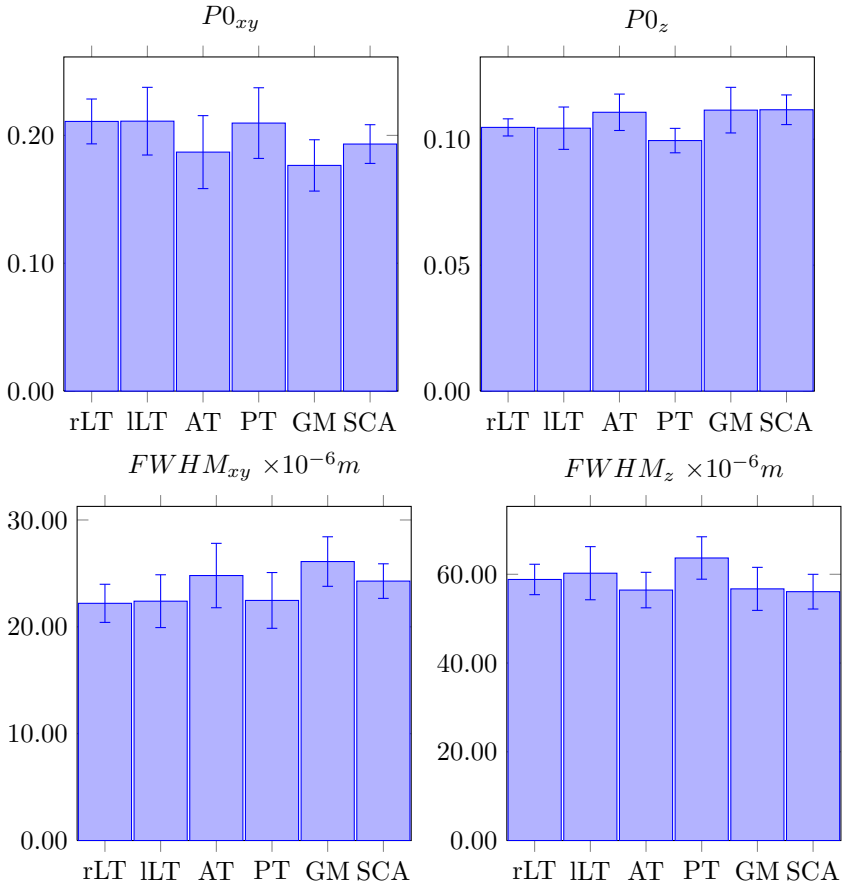

(b) QSI_{xy}& QSI_z metrics

Figure 2.2: Mean and standard deviation of ADC and QSI parameters over all 10 healthy controls for each SC tracts.

Table 2.4: Hotelling's-T^2 significance of pair-wise tract-specific differences ADC_{xy}+ADC_z (confidence interval: 95%)

	lLT	AT	PT	GM
rLT	0.93	**0.04**	**0.03**	***<0.01***
lLT		0.09	0.22	***<0.01***
AT			***<0.01***	0.81
PT				***<0.01***

(a) ADC_{xy},ADC_z

	lLT	AT	PT	GM
rLT	0.44	0.10	0.60	***<0.01***
lLT		0.19	0.92	**0.01**
AT			0.23	0.43
PT				**0.01**

(b) Perpendicular QSI ($P0_{xy}$,$FWHM_{xy}$)

	lLT	AT	PT	GM
rLT	0.57	0.08	**0.02**	**0.04**
lLT		0.22	0.32	0.19
AT			***<0.01***	0.63
PT				**0.01**

(c) Parallel QSI parameters ($P0_z$,$FWHM_z$)

	lLT	AT	PT	GM
rLT	0.71	0.22	0.17	**0.02**
lLT		0.45	0.69	0.08
AT			**0.03**	0.66
PT				**0.02**

(d) Both perpendicular and parallel QSI ($P0_{xy}$,$FWHM_{xy}$,$P0_z$,$FWHM_z$)

Table 2.5: Pearson-correlation coefficient and significance between all ADC and QSI metrics. P-values < 0.01 are displayed as ***bold-italic***.

		ADC_{xy}	ADC_z	$P0_{xy}$	$FWHM_{xy}$	$P0_z$	$FWHM_z$
ADC_{xy}	rho	1.00	0.43	-0.15	-0.25	-0.01	0.15
	p		***<0.01***	***<0.01***	***<0.01***	*0.60*	***<0.01***
ADC_z	rho	0.43	1.00	-0.46	-0.30	0.00	0.21
	p	***<0.01***		***<0.01***	***<0.01***	*0.85*	***<0.01***
$P0_{xy}$	rho	-0.15	-0.46	1.00	-0.05	0.01	0.16
	p	***<0.01***	***<0.01***		***<0.01***	*0.55*	***<0.01***
$FWHM_{xy}$	rho	-0.25	-0.30	-0.05	1.00	0.00	-0.80
	p	***<0.01***	***<0.01***	***<0.01***		*0.92*	***<0.01***
$P0_z$	rho	-0.01	0.00	0.01	0.00	1.00	0.00
	p	*0.60*	*0.85*	*0.55*	*0.92*		*0.84*
$FWHM_z$	rho	0.15	0.21	0.16	-0.80	0.00	1.00
	p	***<0.01***	***<0.01***	***<0.01***	***<0.01***	*0.84*	

2.3 Discussion

Reproducibility

We find overall very good reproducibility of our measurements in both XY and Z. We attribute this to the combination of (i) the small FOV imaging protocol (ii) careful positioning (iii) strong gradient hardware. ADC values are considerably less reproducible than QSI metrics. To some degree this can be explained by the fact that only a subset of the full QSI dataset was used to compute the ADC values. On the other hand, the ADC model is very simple and the number of datapoints we used in this study for ADC fitting should suffice to allow a reliable fit of the mono-exponential decay curve. We assume therefore that the improvement we find in intra-subject reproducibility of QSI over ADC are unlikely just an effect of number of acquisitions alone but rather a feature of the QSI method.

Discrimination of tracts in healthy spinal cord

Both ADC and QSI parameters allow some degree of discrimination between the different ROIs we investigated in this study. In both metrics, GM is most differentiated from all WM regions (except AT). The AT region presents values very similar to those found in the GM region. This can partly be explained by the largest standard deviation of all investigated ROIs. However, it must be noted that the AT is the most difficult ROI to locate due to it's small size. It's size and location makes it hard to delineate from GM in the studied part of the SC. Furthermore, both the AT and GM suffer most from CSF contribution from the anterior median fissure (in case of the AT) and the spinal canal (in case of GM). Therefore the resulting measurements in this region might rather be caused by partial volume effects with CSF and GM (as shown in Chapter 1) than reflect a difference in underlying microstructure of the WM in the AT.

We did not observe any differences between WM regions in the XY direction with neither ADC nor QSI measurements. This is likely an effect of the relatively low gradient strength we used here, which does not allow to distinguish the small axon diameters we expect to find in WM tracts. Considering the relatively long gradient pulse duration of $\delta = 11ms$ used in this study, the centre-of-mass effect described in Section **??** would cause similar contrast for axons smaller than $5\mu m$ (TODO: check!). A further indication of this is the strong correlations between ADC and QSI parameters, which might suggest that the contrast might be governed by the hindered diffusion compartment rather than by differences in restriction.

Interestingly, we found ADC and QSI parameters in Z to be more sensitive to differences between lateral and and posterior tracts. Unlike, XY measurements, diffusion along the long axis of the SC is considered to be predominantly hindered. Henceforth, the observed differences are less likely attributed to differences in axon diameter distributions. Instead, they might inform about other microstructural properties such as the axon packing density or dispersion, which differ between the PT and the LTs. No significant correlation was found between QSI in XY and Z, suggesting that QSI_z provides valuable information on these microstructural properties, which is complementary to the XY measurements.

Finally, we didn't find any advantage of combining multiple QSI parameters in the multi-variate Hotelling-T^2 tests. We suggest this is caused by the redundant information provided by P0 and FWHM parameters describing the dPDF in this clinical setup. This is also supported by the correlations we find between P0 and FWHM in both XY and Z.

Comparision to previous study

The improved study design and image protocol leads to a much reduced variation in both ADC and QSI metrics compared to the previous study (previously variations were found >40% in XY and >16% in Z). Using the better image volume positioning method, we are also more confident in measuring ADC and QSI perpendicular and parallel to the major SC nerve fibres.

Both studies identified significant differences between GM and WM regions. The major difference between the two experiment is the fact that in Experiment 1 we were able to find statistical differences in XY metrics, which we couldn't reproduce in this second study. However, it should be noted that some of those XY findings were suspicious, e.g. showed differences between left and right lateral tract. Although we find less discrimination in XY here, we think the result from this study are more believable. The discrepancies are likely artefactual and stem from different hardware and study designs. Nevertheless, study size is small for both experiments and a larger cohort would be needed to verify the results.

2.4 Conclusion

We have performed two experiments to investigate reproducibility of QSI metrics. We compared QSI metrics with conventional ADC analysis and investigated their ability to discriminate individual WM and GM tracts. For the first time, we also report QSI parameters measured parallel to the SC long axis. In both studies we found better intra- and inter-subject reproducibility in QSI compared to ADC in all investigates ROIs. Furthermore, both QSI and ADC did discriminate GM and WM as well as between some WM ROIs, although QSI metrics did not increase the differences significantly. Furthermore, we found that measurements in Z helped to distinguish structural differences of WM tracts with more accuracy, and complemented ADC and QSI values in XY direction.

The encouraging initial results described in Chapter1 motivated this second study, in which we tackled some of the major limiting factors of the first Experiments, in particular low gradient strength and low spatial resolution. We confirmed the general trends found in intra- and inter-subject reproducibility, although overall reproducibility was reduced in all metrics as an effect of the optimised imaging protocol. However, we were able to confirm in this experiment that ADC and QSI metrics in Z provides useful information about the microstructure parallel to the principle fibre direction. The low standard deviation of QSI in this study makes our QSI protocol attractive for clinical studies, as it would help reducing sample numbers to detect differences e.g. in patient cohort as in (Farrell et al., 2008).

Bibliography

Assaf, Y., Ben-Bashat, D., Chapman, J., & Peled, S. (2002). High b-value q-space analyzed diffusion-weighted MRI: Application to multiple sclerosis. *Magnetic Resonance in Medicine*.

Assaf, Y., Mayk, A., & Cohen, Y. (2000). Displacement imaging of spinal cord using q-space diffusion-weighted MRI. *Magnetic Resonance in Medicine*.

Avram, L., Assaf, Y., & Cohen, Y. (2004). The effect of rotational angle and experimental parameters on the diffraction patterns and micro-structural information obtained from q-space diffusion nmr: implication for diffusion in white matter fibers. *Journal of Magnetic Resonance*, *169*(1), 30–38.
URL `http://www.sciencedirect.com/science/article/pii/S1090780704000850`

Bar-Shir, A., Avram, L., Ozarslan, E., Basser, P. J., & Cohen, Y. (2008). The effect of the diffusion time and pulse gradient duration ratio on the diffraction pattern and the structural information estimated from q-space diffusion MR: experiments and simulations. *Journal of Magnetic Resonance*, *194*(2), 230–236.

Cohen, Y., & Assaf, Y. (2002). High b-value q-space analyzed diffusion-weighted MRS and MRI in neuronal tissues – a technical review. *NMR in Biomedicine*.

Farrell, J. A. D., Smith, S. A., Gordon-Lipkin, E. M., Reich, D. S., Calabresi, P. A., & van Zijl, P. C. (2008). High b-value q-space diffusion-weighted MRI of the human cervical spinal cord in vivo: feasibility and application to multiple sclerosis. *Magnetic Resonance in Medicine*, *59*(5), 1079–1089.

Freund, P. A. B., Dalton, C., Wheeler-Kingshott, C. A. M., Glensman, J., Bradbury, D., Thompson, A. J., & Weiskopf, N. (2010). Method for simultaneous voxel-based morphometry of the brain and cervical spinal cord area measurements using 3D-MDEFT. *Journal of magnetic resonance imaging : JMRI*, *32*(5), 1242–7.
URL `http://www.pubmedcentral.nih.gov/articlerender.fcgi?artid=3078516&tool=pmcentrez&rendertype=abstract`

Hesseltine, S. M., Law, M., Babb, J., Rad, M., Lopez, S., Ge, Y., Johnson, G., & Grossman, R. I. (2006). Diffusion tensor imaging in multiple sclerosis: assessment of regional differences in the axial plane within normal-appearing cervical spinal cord. *AM J NEURORADIOL*, *27*(6), 1189–1193.

Horsfield, M. A., Sala, S., Neema, M., Absinta, M., Bakshi, A., Sormani, M. P., Rocca, M. A., Bakshi, R., & Filippi, M. (2010). Rapid semi-automatic segmentation of the spinal cord from magnetic resonance images: application in multiple sclerosis. *NeuroImage*, *50*(2), 446–455.

Lätt, J., Nilsson, M., Malmborg, C., Rosquist, H., Wirestam, R., Stå hlberg, F., Topgaard, D., & Brockstedt, S. (2007). Accuracy of q-space related parameters in MRI: simulations and phantom measurements. *IEEE Transactions on Medical Imaging*, *26*(11), 1437–1447.

Ong, H. H., & Wehrli, F. W. (2010). Quantifying axon diameter and intracellular volume fraction in excised mouse spinal cord with q-space imaging. *NeuroImage*, *51*(4), 1360–1366.
URL `http://www.ncbi.nlm.nih.gov/pmc/articles/PMC2895496/`

Ong, H. H., Wright, A. C., Wehrli, S. L., Souza, A., Schwartz, E. D., Hwang, S. N., & Wehrli, F. W. (2008). Indirect measurement of regional axon diameter in excised mouse spinal cord with q-space imaging: simulation and experimental studies. *NeuroImage*, *40*(4), 1619–1632.

Schneider, T., Ciccarelli, O., Kachramanoglou, C., Thomas, D. L., & Wheeler-Kingshott, C. A. M. (2011). Reliability of tract-specific q-space imaging metrics in healthy spinal cord. In *Proceedings 19th Scientific Meeting, International Society for Magnetic Resonance in Medicine*.

Wilm, B., Svensson, J., Henning, A., Pruessmann, K., Boesiger, P., & Kollias, S. (2007). Reduced field-of-view mri using outer volume suppression for spinal cord diffusion imaging. *Magnetic Resonance in Medicine*, *57*(3), 625–630.
URL `http://onlinelibrary.wiley.com/doi/10.1002/mrm.21167/abstract`